Eur. Phys. J. B **3**, 155–161 (1998)

THE EUROPEAN PHYSICAL JOURNAL B

Sonic stop-bands for cubic arrays of rigid inclusions in air

M.S. Kushwaha[a], B. Djafari-Rouhani, L. Dobrzynski, and J.O. Vasseur

Laboratoire de Dynamique et Structures des Matériaux Moléculaires[b], U.F.R. de Physique, Université de Lille I, 59655 Villeneuve d'Ascq Cedex, France

Received: 24 October 1997 / Revised: 1 December 1997 and 26 January 1998 / Accepted: 6 March 1998

Abstract. Extensive band structures have been computed for cubic arrays of rigid spheres and cubes in air. Complete stop bands are obtained for the face-centered-cubic (fcc) structure; however, there is no gap for the body-centered-cubic (bcc) and simple-cubic (sc) structures. These gaps start opening up for a filling fraction of $\approx$ 54% (27%) for spherical (cubic) inclusions and tend to increase with the filling fraction, exhibiting a maximum at the close-packing. We also propose a tandem structure that allows the achievement of an ultrawideband filter for environmental or industrial noise in the desired frequency range. This work is motivated by the recent experimental measurement of sound attenuation on the sculpture, by Eusebio Sempere, exhibited at the Juan March Foundation in Madrid (Nature **378**, 241 (1995)) and complements the corresponding theoretical work (Appl. Phys. Lett. **70**, 3218 (1997)).

PACS. 43.40.+s Structural acoustics and vibration – 63.20.-e Phonons in crystal lattices – 42.45.Fx Diffraction and scattering

1 Introduction

An architectural proposal of Yablonovitch [1] and a conceptual hypothesis of Sajeev John [2] triggered the primary interest in photonic crystals. These are periodic dielectric structures that exhibit a band gap, by analogy with the electronic band gap in semiconductor crystals. Within these photonic band gaps, the atoms are denied spontaneously absorbing and re-emitting light; this has signalled practical interest to produce highly efficient lasers. From the fundamental point of view, the existence of complete or pseudo gaps in a weakly disordered system is paramount in determining the transport properties and realizing the Anderson localization of light. Since the prominent phenomena emerging from the physics of photonic crystals are all consequences of the existence of a photonic band gap, much of the research effort has been dedicated to the search for such photonic crystals [3].

Within a few years of the emergence of photonic crystals, a growing interest in the analogous studies on "phononic crystals" has been seen [4–17]. These are the two- and three-dimensional periodic elastic/acoustic composites that exhibit spectral gaps in the band structure. In analogy to the photonic crystals, the prime interest of the band theorists has been the occurrence of *complete* elastic/acoustic band gaps (or stop bands). The term complete refers to the gaps which exist independent of the polarization of the wave as well as its direction of propagation. Within these gaps the sound, vibrations and phonons are all forbidden. This is of interest for applications such as elastic/acoustic filters, improvements in the design of transducers, and noise control; as well as for pure physics concerned with the Anderson localization of sound and vibrations [18,19]. Piezoelectric and piezomagnetic composites are already known to have long standing applications as medical ultrasonics and naval transducers; as well as for related tasks in medical imaging [20,21]. Such composites were initially fabricated for sonar applications and are now widely used for ultrasonic transducers.

It is interesting to remark that in all *artificial* periodic structures –dielectric composites, elastic composites, magnetic composites, *etc.*– the existence of *complete* gaps is attributed to the joint effect of the Bragg diffraction and the Mie scattering. The destructive interference due to Bragg diffraction accompanied by the Mie resonances due to strong scattering from individual spheres is the conceptual base of the complete gaps. The latter becomes effective when the diameter of the sphere is close to an integer multiple of wavelength [3].

In the quest for achieving complete gaps one must resort to the band structure calculations. These have been performed for several geometries of periodic elastic composites and for various types of waves [4–17]. One-dimensional (1D) periodic systems (superlattices, for example) allow longitudinal, transverse, and mixed modes. Two-dimensional (2D) composites permit the propagation of pure transverse and mixed modes independently; no longitudinal modes are possible, however. In

[a] *Permanent address*: Institute of Physics, University of Puebla, Box J–48, Puebla 72570, Mexico.
e-mail: `manvir@sirio.ifuap.buap.mx`

[b] URA CNRS No. 801

three-dimensional (3D) composites the longitudinal and transverse modes are strongly coupled, thus complicating the nature of the eigenmodes and the corresponding computation. A drastic simplification arises in the case of liquids and gases, which support only dilatational (acoustic) waves. In what follows we will be concerned with such a single polarization of dilatational waves.

The present work is motivated by the recent experimental measurements of sound attenuation on the sculpture, by Eusebio Sempere, exhibited at the Juan March Foundation in Madrid [22]. It consists of a periodic distribution of hollow stainless steel cylinders, with diameter of 2.9 cm and a unit cell of edge 10 cm. The cylinders are fixed on a circular platform (4 m in diameter) which can rotate on a vertical axis. The sound attenuation was measured in the outdoor conditions for the wave-vectors perpendicular to the cylinders' vertical axis. The sculpture thus corresponds to a cermet topology with a volume fraction occupied by the scatterers of 0.066 and a sound-speed ratio of 17.9. The experimentalits' speculation, based on their observation, was that the sound attenuation peak at 1.67 kHz could be ascribed to the formation of the first (*i.e.*, the lowest) gap in this sculpture. We call attention to two important points: first, the sculpture represents a 2D periodicity in the $x-y$ plane (provided the cylinders' vertical axis is presumed to be along the z-axis); second, the sculpture consists of finite (in length) cylinders and is not strictly periodic (in the sense that it does not extend infinitely in the $x-y$ plane).

This experimental finding was soon followed by a rigorous theoretical investigation embarking on the *ideal* situation and employing the actual experimental parameters (we refer to the true dimensions of the sculpture) [23]. The complete band structure and density of states (DOS) were computed for an ideal 2D periodic system to draw the following conclusions. It was found that for the experimental situation (*i.e.*, for the cylinders 2.9 cm in diameter and system-period of 10 cm implying the filling fraction $f = 0.066$) there is *no* acoustic gap for frequencies below 6.4 kHz. However, the DOS reveal promiment minima at 1.7 and 2.4 kHz. These frequencies do agree with those of the first two attenuation maxima in reference [22], and are indeed related to the diffraction from [100] and [110] planes (*i.e.*, the $\overline{X}$ and $\overline{M}$ high symmetry points in the Brillouin zone). Thus, *even with idealization*, Sempere's sculpture was seen to exhibit only pseudogaps – *not full gaps*. We refer the readers to reference [23] for other details regarding the circumstances where such a sculpture could exhibit complete gaps. It is noteworthy that the term complete was reserved in the sense that both experiment and theory ignored the possibility of filtration of sound along the vertical axis of the cylinders.

In this work, we consider a 3D geometry of rigid (for example, stainless steel) spheres and cubes in a rarer medium (for example, air) – analogous to Eusebio Sempere's sculpture in mind. In a sense, this complements the previous work on 2D systems in reference [23] to investigate whether or not there could exist a *complete* gap in the realistic situation of 3D systems. It has been found that an fcc system gives rise to a genuine stop band, whose frequency range can be raised (lowered) by decreasing (increasing) the period of the system. However, bcc and sc structures do not exhibit any gap at least as far as the 50th band. The details of the theory of band structure for elastic/acoustic composites of arbitrary periodicity and inhomogeneity can be found in reference [7]. However, the methodological details needed to accomplish the problem at hand are described succinctly in the following section.

2 Formalism

We consider a 3D periodic system made up of *infinitely* rigid spheres and cubes in air – with fcc, bcc, and sc structures. The assumption of infinite rigidity means the modulus of compressibility of the inclusions is infinite. However, in order to keep the usual speed of sound, we are brought to assume that the density of the inclusions is also infinite. This hypothesis, which is very well justified for the metallic (for example, stainless steel) inclusions in air, then implies that the sound does not penetrate such inclusions, and hence the propagation is confined and predominantly only in the air. In other words there is no communication between the air inside and outside. Then it really does not matter whether these inclusions are hollow or solid within. Therefore, the calculation at hand simplifies considerably because the transverse speed of sound c_t is zero in gases (and liquids). Nevertheless, the ordinary wave equation is inapplicable to the inhomogeneous media. The correct wave equation – simply the equation of motion in the absence of an external force – is

$$\rho \frac{\partial^2 \mathbf{u}}{\partial t^2} = \boldsymbol{\nabla}(\rho c_l^2 \boldsymbol{\nabla} \cdot \mathbf{u}), \tag{1}$$

where $\rho(\mathbf{r})$ is the mass density and $c_l(\mathbf{r})$ is the longitudinal speed of sound. Only if ρc_l^2 is independent of the position, do all the three components of $\mathbf{u}(\mathbf{r}, t)$ satisfy the ordinary wave equation. In the general case, we observe, from equation (1), that $\boldsymbol{\nabla} \times (\rho \mathbf{u}) = 0$. Hence it is possible to define a scalar potential $\Phi(\mathbf{r}, t)$ such that $\rho \mathbf{u} = \boldsymbol{\nabla} \Phi$. Then equation (1) may be cast in the form

$$(C_{11})^{-1} \frac{\partial^2 \Phi}{\partial t^2} = \boldsymbol{\nabla} \cdot (\rho^{-1} \boldsymbol{\nabla} \Phi) \tag{2}$$

where $C_{11} = \rho c_l^2$ is the longitudinal elastic constant. Taking advantage of the 3D periodicity, we expand the quantities $\rho^{-1}(\mathbf{r})$ and $C_{11}^{-1}(\mathbf{r})$ in the Fourier series:

$$\rho^{-1}(\mathbf{r}) = \sum_{\mathbf{G}} \sigma(\mathbf{G}) e^{i\mathbf{G}\cdot\mathbf{r}},$$
$$C_{11}^{-1}(\mathbf{r}) = \sum_{\mathbf{G}} \zeta(\mathbf{G}) e^{i\mathbf{G}\cdot\mathbf{r}} \tag{3}$$

where $\mathbf{G}$ and $\mathbf{r}$ are the 3D reciprocal and direct lattice vectors. The solution of equation (2) is given by means of the Bloch theorem:

$$\Phi(\mathbf{r}, t) = e^{i(\mathbf{K}\cdot\mathbf{r} - \omega t)} \sum_{\mathbf{G}} \Phi_{\mathbf{K}}(\mathbf{G}) e^{i\mathbf{G}\cdot\mathbf{r}}. \tag{4}$$

Here $\mathbf{K}$ is a 3D Bloch vector. With the aid of equations (3, 4), equation (2) yields an infinite set of equations for eigenvalues $\omega(\mathbf{K})$ and eigenvectors $\Phi_{\mathbf{K}}(\mathbf{G})$:

$$\sum_{\mathbf{G}'} \left[\sigma(\mathbf{G}-\mathbf{G}')(\mathbf{K}+\mathbf{G})\cdot(\mathbf{K}+\mathbf{G}') - \zeta(\mathbf{G}-\mathbf{G}')\omega^2\right] \times \Phi_{\mathbf{K}}(\mathbf{G}') = 0. \quad (5)$$

We apply this equation to a periodic system of spherical and cubic inclusions (medium i) in a background (medium b); the filling fraction of the spheres/cubes is f. The corresponding densities (elastic constants) are $\rho_i, \rho_b(C_{11i}, C_{11b})$. Then it is a simple matter to show that [7]

$$\sigma(\mathbf{G}) = \begin{cases} \rho_i^{-1} f + \rho_b^{-1}(1-f) \equiv \overline{\rho^{-1}}, & \text{for } \mathbf{G}=0 \\ (\rho_i^{-1} - \rho_b^{-1}) F(\mathbf{G}) \equiv \Delta(\rho^{-1}) F(\mathbf{G}), & \text{for } \mathbf{G}\neq 0 \end{cases} \quad (6)$$

where the structure factor $F(\mathbf{G})$ is given by

$$F(\mathbf{G}) = \frac{1}{V_c}\int_i d^3 r e^{-i\mathbf{G}\cdot\mathbf{r}} = \begin{cases} \frac{3f}{(Gr_0)^3}[\sin(Gr_0) - (Gr_0)\cos(Gr_0)] \\ \frac{f}{(G_x l/2)(G_y l/2)(G_z l/2)} \sin(G_x l/2)\sin(G_y l/2)\sin(G_z l/2). \end{cases} \quad (7)$$

The first (second) expression in equation (7) corresponds to the spherical (cubic) inclusions. V_c is the volume of the unit cell, the integration is limited to a sphere (cube) of radius (side) r_0 (l), and the filling fraction $f = n(4\pi/3)r_0^3/V_c$ (nl^3/V_c) for spherical (cubic) inclusions; where n refers to the number of spheres (cubes) in the unit cell. An equation analogous to equation (6) can be written for $\zeta(\mathbf{G})$ in terms of C_{11}^{-1}. Then equation (5) can be cast in the form

$$\sum_{\mathbf{G}'\neq\mathbf{G}} F(\mathbf{G}-\mathbf{G}') \times \left[\Delta(\rho^{-1})(\mathbf{K}+\mathbf{G})\cdot(\mathbf{K}+\mathbf{G}') - \Delta(C_{11}^{-1})\omega^2\right]\Phi_{\mathbf{K}}(\mathbf{G}') + \left[\overline{\rho^{-1}}\,|\mathbf{K}+\mathbf{G}|^2 - \overline{C_{11}^{-1}}\omega^2\right]\Phi_{\mathbf{K}}(\mathbf{G}) = 0. \quad (8)$$

Interestingly, this eigenvalue equation for dilatational modes is formally the same as the eigenvalue equation for *transverse* modes in the corresponding solid composites with 2D periodicity (see, for example, Eq. (6) in Ref. [5]). It is not difficult to rewrite equation (8) in the form of a standard eigenvalue problem [7], which is in fact performed at the computational level. Doing so ensures a drastic saving in computational time.

For the purpose of computation, we limited the number of plane waves to 343. This resulted in a reliably very good convergence; at least up to the lowest 20 bands. By increasing the number of plane waves to 729, our results change, after the 20th band, by less than 1%. This emboldens our confidence in the adequacy of our results based on the 343 plane waves, particularly in the low-frequency regime where the *complete* stop bands were found.

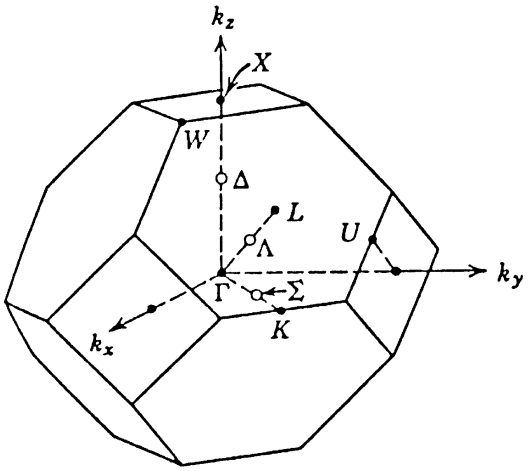

Fig. 1. The first Brillouin zone (a truncated octahedron) of the face-centered-cubic lattice showing the symmetry points and axes.

Note that our numerical results, presented in the following section, correspond specifically to the composite system made up of stainless steel inclusions in air. However, the results remain quite unaltered if we impose the conditions of infinite rigidity (see above). This is clearly an artifact of the huge contrast in the material parameters of the inclusions and the background.

3 Results and discussion

Figure 1 depicts the first Brillouin zone for the fcc structure which is of immediate relevance for the work reported in this paper.

Figure 2 illustrates the band structure and the density of states (DOS) for rigid spheres in a fcc structure; for a filling fraction of $f = 0.65$. The lowest *ten* bands are depicted. The plots are rendered in terms of the eigenfrequency $\nu = \Omega(2\pi\overline{c}_l/a)$ (where a is the lattice constant and $\overline{c}_l = \sqrt{(\overline{\rho^{-1}}/\overline{C_{11}^{-1}})}$) *vs.* dimensionless Bloch vector $\mathbf{k} = \mathbf{K}a/2\pi$. The left part of the triptych represents the band structure in the five principal symmetry directions, letting $\mathbf{k}$ scan only the periphery of the irreducible part of the first Brillouin zone (see Fig. 1). The middle part is the result of an extensive scanning of $|\mathbf{k}|$ in the irreducible part of the Brillouin zone – the interior of this zone and its surface, as well as the principal directions shown in the left part of the figure. Each curve here corresponds to some direction of $\mathbf{k}$. The DOS in the right part of the triptych has been calculated on the basis of the scanning in the middle part, which corresponds to 1300 $\mathbf{k}$–points within the irreducible part of the first Brillouin zone. The three parts of the triptych in Figure 2 together demonstrate that there is, indeed, a genuine, complete gap (the shaded region) existing between the first and *second* bands; and we consider such calculations as essential. It should be pointed out that the crossing of the second and third bands within the ΓX direction apparently leads one to have an impression that it is the minimum (at X point)

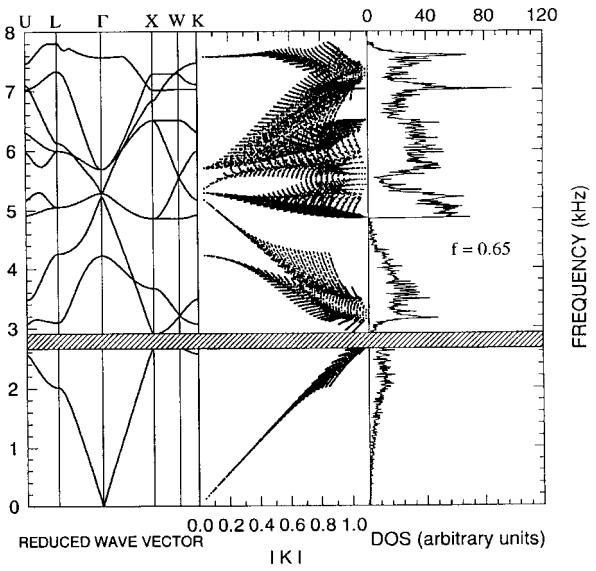

Fig. 2. Acoustic band structure and density of states for a fcc array of *rigid* spheres in air.The plots are rendered in terms of the frequency $\nu = \Omega(2\pi\overline{c}_l/a)$ [where a is the lattice constant and $\overline{c}_l = \sqrt{(\overline{\rho^{-1}}/\overline{C_{11}^{-1}})}$] *vs.* dimensionless Bloch vector $\mathbf{k} = \mathbf{K}a/2\pi$. The filling fraction is $f = 0.65$. and the period is $a = 10$ cm. The triptych is comprised of three parts: In the left panel, we plot the band structure in the five principal symmetry directions, letting the Bloch vector $\mathbf{k}$ scan only the periphery of the irreducible part of the first Brillouin zone. The middle panel demonstrates a novel way of plotting the eigenvalues as a function of $|\mathbf{k}|$; *i.e.*, the distance of a point in the irreducible part of the Brillouin zone from the Γ point. The right panel illustrates the DOS. We call attention to the complete stop–band (hatched region) extending throughout the Brillouin zone.

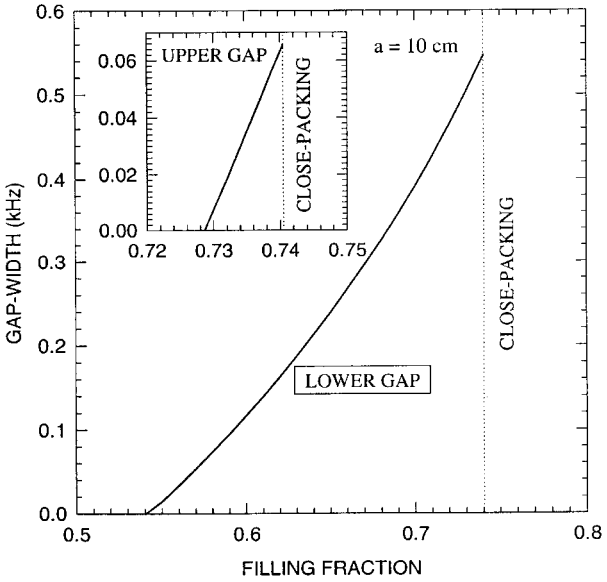

Fig. 3. Gap–widths of the only existing two stop–bands *vs.* filling fraction for a fcc array of *rigid* spheres in air. The period of the system (*i.e.*, the lattice constant) $a = 10$ cm. The vertical dotted line refers to the close–packing value ($f = 0.7405$). Evident is the fact that there is no acoustic stop–band for $f \leq 54\%$. The inset depicts the upper stop band that opens up for $f \geq 0.7287$.

of the third band which is the top of the stop band. However, since one always intends to count the bands (in the increasing order of frequency) from the bottom, we prefer to call the top of the stop band as the minimum of the second band. We notice that there is *no other* band gap existing at least up to the 50th band. We did not find any gap for bcc and sc structures. Note that the existing band gap in an fcc lattice is an indirect one in the language of Solid State physics – with the minimum (maximum) of the second (first) band lying at the high symmetry point X (W) in the Brillouin zone.

Next we plot the gap–widths of the two existing stop bands within the first ten bands in the fcc structure in Figure 3. The size of a complete gap is usually expressed as the ratio of the gap-width and the midgap frequency. The gap–width on the y-axis represents just a difference in frequencies of the top and bottom of the stop band, for a given filling fraction. As seen from the figure, the filling fraction must exceed a certain minimum value, f_{min}, for a gap to be opened. This leads us to infer that there is no band gap for $f_{min} < 0.54$. The largest band gap occurs at the close–packing when the spheres fill approximately 74% of the space (with $f_{max} = \pi/\sqrt{18}$, to be precise). It is observed that, at the close-packing, the bands become relatively flatter and give rise to *two* complete stop bands – the lower one is the same between first and second bands, and the upper one occurs between the third and the fourth bands. The latter is also an indirect gap – defined by the maximum of the third band at the Γ-point and the minimum of the fourth band at the X-point. The upper band gap starts at $f = 0.7287$ and increases with the filling fraction, just as the lower gap. The upper gap is smaller (than the lower one) but it is also a complete gap. The gap/midgap ratio in the limit of close-packing is found to be 0.21 (0.013) for the lower (upper) gap.

That the fcc–lattice–arrangement allows the densest packing when the spheres are crammed together, is true. However, it is noteworthy that *not all* the spheres "kiss" each other in the limit of close–packing – all the four spheres at the corners of *a face* touch the one at the center of this face (of a unit cell), but each of them remains apart from its six next–nearest neighbors by a distance of $\approx 29\%$ of the lattice constant. That implies that even the fcc arrangement does not allow truly isolated vortices and hence the sound can still spin around the rigid spheres in the background medium (be it air or water). This is the reason that the fcc geometry can (and does) allow an *almost* normal band structure in the limit of close-packing, unlike the discrete bands in the 2D square lattice.

Finally we propose the fabrication of a multiperiodic system in tandem that could be designed so as to give rise to wider stop bands in the *desired* frequency range. We compute the band–gap edges of the lowest, which is also the widest, stop band as a function of the filling fraction for a large number of systems with different periods

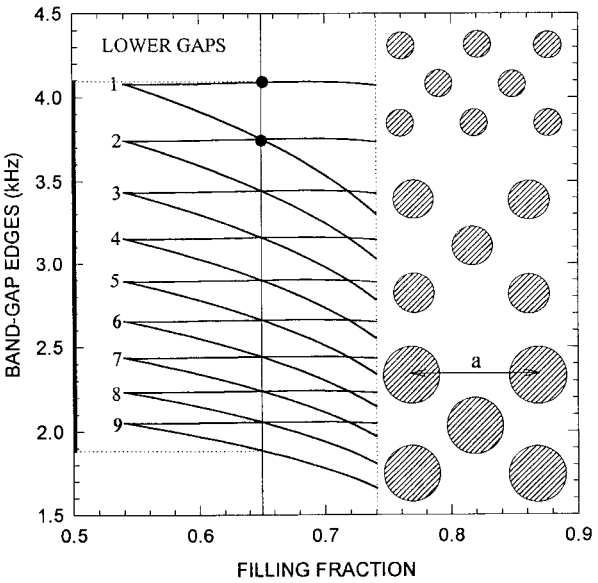

Fig. 4. Inset: cross-section of a tandem structure of (periodic) cubic arrays of *rigid* spheres in fcc arrangement– what is shown is the front face of a unit cell of an individual periodic system. The "wedges" numbered 1–9 correspond, respectively, to the periods of 7.09, 7.72, 8.42, 9.17, 10.00, 10.89, 11.87, 12.94, and 14.10 cms. Each of the nine sets produces a stop band, whose upper and lower edges are plotted as a function of the filling fraction f. For $f = 0.65$ (vertical solid line), the nine stop bands join precisely so as to form a "super stop band" within a frequency between 1.88 kHz and 4.09 kHz (see the bold vertical frequency bar between the two horizontal dotted lines). The vertical dotted line refers to the close–packing value $f = 0.7404$. This is the most convenient way of demonstrating the existence of stop–bands in a given periodic system.

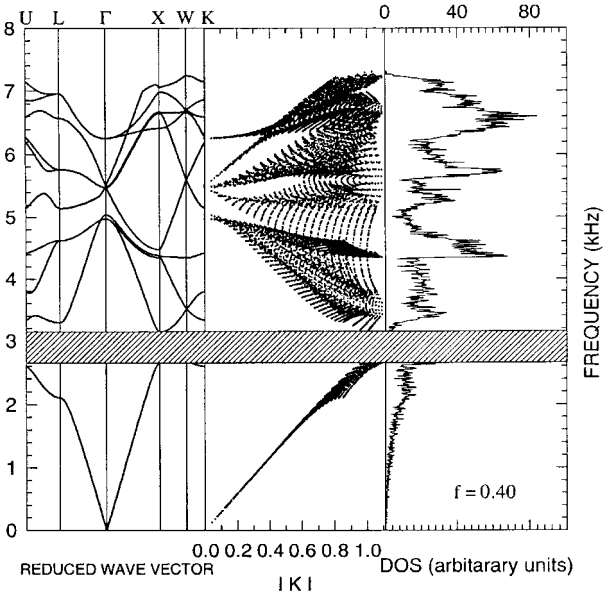

Fig. 5. The same as in Figure 1, but for a fcc array of *rigid* cubes in air. The filling fraction is $f = 0.40$ and the period is $a = 10$ cm. The hatched region refers to the complete stop band extending throughout the Brillouin zone.

(the lattice constants). The numerical results of such investigations are illustrated in Figure 4. The "wedges" labeled 1 to 9 correspond to different periods (in increasing order from top to bottom) and are based on the numerous band structure calculations– one for every value of the filling fraction f. These are really eigenvalue problems for the reduced frequency Ω as a function of the Bloch vector $\boldsymbol{k}$ scanned in all directions. It is important to note here (and, in fact, throughout this paper) that the eigenfrequency ν is inversely proportional to the period of the system. That means that, given the specific medium in the background, the frequencies of a "wedge" for a period of 1 cm will be 10 times higher than those of a "wedge" corresponding to a period of 10 cm. Consider two dots on "wedge" # 1 for a filling fraction $f = 0.65$. The dots mark the upper and lower edges of the stop band in the band structure and the vertical distance between them is the width of the stop band. Now we calculate the ratio of the two frequencies (specified by the dots) and create the next "wedge" # 2 such that its upper edge (at the same f) crosses the lower edge of "wedge" # 1. The same procedure is repeated for all the nine "wedges" depicted in Figure 4. In fact, we start with "wedge" # 5 that corresponds to a period of $a = 10$ cm. We embark on the optimum situation which refers to the lesser possible number of periodic composites and the smaller possible filling fraction – the former point concerns the cost and the latter hints to eventually avoiding construction of a wall of rigid spheres. We appeal to the filling fraction $f = 65\%$, where only nine 3D periodic composites in fcc are enough to guarantee a "super stop band" from 1.88 kHz to 4.09 kHz. The range of the "super stop band" is high-lighted by a bold vertical frequency bar in Figure 4. Within the "super stop band" the multiperiodic system (designed in tandem) stands still and total silence reigns. By this we mean that if one tries to transmit a wide-band wave through the tandem structure one will achieve a zero transmission within the range of the "super stop band". The completeness of such a "super stop band" is assured due to the overlapping of the individual stop bands in the neighboring composites. However, the frequency range of such a "super stop band", as mentioned above, is at the will of the designer – by increasing (decreasing) the period of the composites one can lower (raise) the frequency range of the stop bands and hence of the "super stop band".

Similar calculations were performed for cubic inclusions in the fcc, bcc, and sc structures. Again the bcc and sc structures did not exhibit any stop bands. The analogous results for the fcc structure are displayed in Figures 5-7. Figure 5 displays the band structure and DOS for $f = 0.40$. There is a complete stop band from 2.65 kHz to 3.14 kHz within the first ten bands. Figure 6 depicting the variation of the gap-width with the filling fraction dictates that there is no gap for $f < 27.4\%$. We remark that no other gap was found at least up to the 50th band. The gap/midgap ratio in the limit of close-packing ($f = 0.50$) is found to be 0.4; *i.e.*, almost double of that achieved

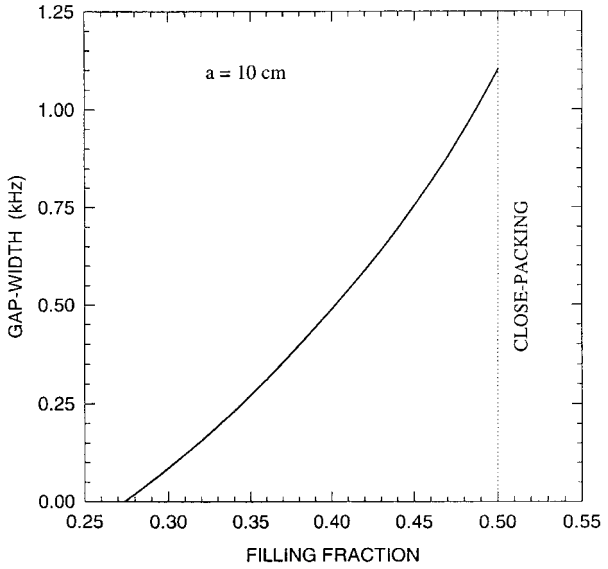

Fig. 6. Gap–widths of the only existing stop–band vs filling fraction for a fcc array of *rigid* cubes in air. The period of the system is $a = 10$ cm. The vertical dotted line refers to the close–packing value ($f = 0.50$). Clearly, there is no stop–band for $f < 27.4\%$.

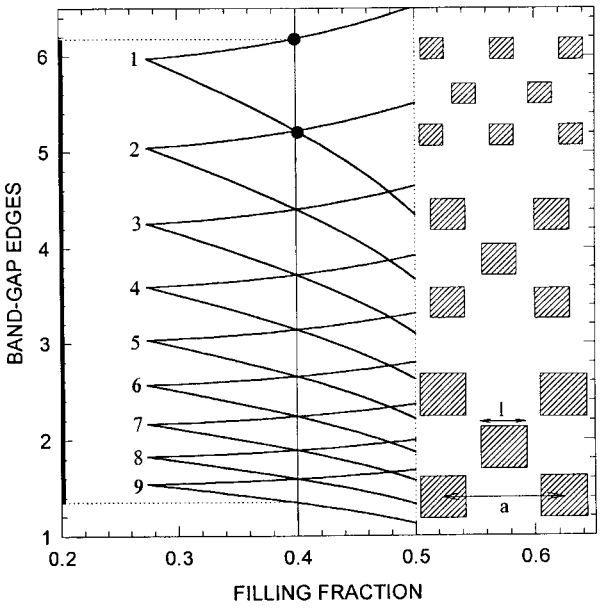

Fig. 7. The same as in Figure 4, but for a fcc array of *rigid* cubes in air. The "wedges" numbered 1–9 correspond, respectively, to the period of 5.08, 6.02, 7.13, 8.44, 10.00, 11.84, 14.02, 16.60, and 19.66 cms. Each of the nine sets produces a stop band, whose upper and lower edges are plotted as a function of the filling fraction f. For $f = 0.40$ (vertical solid line), the nine stop bands join precisely so as to form a "super stop band" within a frequency range between 1.35 kHz and 6.18 kHz (see the bold vertical frequency bar between the two horizontal dotted lines). The vertical dotted line refers to the close–packing value $f = 0.50$.

from the lower gap in the case of spherical inclusions. Figure 7 demonstrates the design of the "super stop band" within the frequency range between 1.35 and 6.18 kHz, for $f = 0.40$, in the tandem structure made up of nine 3D periodic composites in fcc. The essential difference, as compared to the spherical inclusions, is that the band gaps are larger and these are opened at relatively lower filling fractions. From the technological point of view, this has an obvious advantage of designing ultrawideband filters for noise with relatively lesser number of 3D composites with large periods; and this is because of the lower filling fractions serving the purpose. The rest of the discussion related to the corresponding Figures 1-3 is still valid.

4 Summary

To conclude with, using simple mathematical tools employing the theory of elasticity, we have demonstrated that a 3D periodic system of rigid spherical and cubical inclusions in fcc arrangement can give rise to complete stop bands. We see that a minimal filling fraction $f \approx 54\%$ (27%) is needed for the obtention of a forbidden band for the spherical (cubic) inclusions in the fcc structure. The 3D tandem structures proposed here could be designed to achieve large "super stop bands" within the desired frequency range. The frequency range of such "super stop bands" can be raised (lowered) by decreasing (increasing) the period (or lattice constant) of the constituent systems. In analogy to the photonic and phononic cases, in the frequency range of stop bands sound and vibrations would be forbidden. Thus a small vibrator (or defect) introduced into an otherwise periodic system would remain unable to generate sound within the gaps. The weakly disordered system should, on the contrary, exhibit localized modes within the gaps. The existence of complete stop bands is thus closely associated with the Anderson localization of sound and vibrations. Note that neither bcc nor sc structures are found to exhibit any gap for either of the two shapes of the inclusions.

It is noteworthy that the existence of a complete gap in these "phononic crystals" guarantees the perfect reflection (and hence no transmission) of the excited acoustic wave within the frequency range of the stop band. But this does not mean that the intensity of the backscattered part of the incoming wave vanishes. The technological interest behind fabricating such "phononic crystals" is to enable the medium to prohibit the incoming wave within a desired (or tailor-made) forbidden frequency range. Consequently, such periodic composites that exhibit complete stop bands can behave as acoustic filters that prohibit sound propagation at certain frequencies while allowing practically free (provided that the absorption is scaled down to a minimum) propagation at others.

Figures 4 and 7 address indirectly a typical question concerned with the strategy of unwanted noise abatement: Is it feasible to devise low–tech means that can forbid the sound propagation in the human audible range of frequencies (20 Hz – 20 kHz)? This is a very important question that has become a major concern of scientists, engineers,

and architects, involved in the design of buildings and in the planning of cities, working together to find technically feasible solutions to the problem of noise. Fundamental to bringing about a solution is a better understanding of sound propagation through city streets and in the atmosphere above a city. For such an understanding the availability of band structures is essential. This letter is simply meant to emphasize the fundamental issues involved in the sister subject of band–gap engineering of periodic composite systems. Our theoretical results suggest the feasibility of designing an ultrawideband filter for environmental or industrial noise in air (or water) according to the required specifications.

One of us (M.S.K.) gratefully acknowledges the hospitality of the Laboratoire de Dynamique et Structure des Matériaux Moléculaires, URA CNRS No. 801, University of Lille I. He would also like to express his sincere thanks to the "Ministère de l'Éducation, de la Recherche et de la Technologie" and to the "Conseil Régional Nord-Pas de Calais" for the financial support. This work was partially supported by CONACYT, Mexico, Grant # 2373–PE. M.S.K. feels thankful to Mr. A. Khelif for occasional technical help with the software.

References

1. E. Yablonovitch, Phys. Rev. Lett. **58**, 2059 (1987).
2. Sajeev John, Phys. Rev. Lett. **58**, 2486 (1987).
3. For a recent extensive review, see M.S. Kushwaha, Int. J. Mod. Phys. B **10**, 977 (1996).
4. A.A. Ruffa, J. Acoust. Soc. Am. **91**, 1 (1992); M.M. Sigalas, E.N. Economou, J. Sound Vib. **158**, 377 (1992).
5. M.S. Kushwaha, P. Halevi, L. Dobrzynski, B. Djafari–Rouhani, Phys. Rev. Lett. **71**, 2022 (1993).
6. M. Sigalas, E.N. Economou, Solid State Commun. **86**, 141 (1993).
7. M.S. Kushwaha, P. Halevi, G. Martinez, L. Dobrzynski, B. Djafari–Rouhani, Phys. Rev. B **49**, 2313 (1994).
8. M.S. Kushwaha, P. Halevi, Appl. Phys. Lett. **64**, 1085 (1994).
9. J.O. Vasseur, B. Djafari–Rouhani, L. Dobrzynski, M.S. Kushwaha, P. Halevi, J. Phys. Condens. Matter **6**, 8759 (1994).
10. E.N. Economou, M.M. Sigalas, J. Acoust. Soc. Am. **95**, 1735 (1994).
11. M.S. Kushwaha, P. Halevi, L. Dobrzynski, B. Djafari–Rouhani, Phys. Rev. Lett. **75**, 3581 (1995).
12. M. Kafesaki, M.M. Sigalas, E.N. Economou, Solid State Commun. **96**, 285 (1995).
13. S. Parmley, T. Zobrist, T. Clough, A. Perez–Miller, M. Makela, R. Yu, Appl. Phys. Lett. **67**, 777 (1995).
14. M.S. Kushwaha, P. Halevi, Appl. Phys. Lett. **69**, 31 (1996).
15. M.S. Kushwaha, B. Djafari–Rouhani, J. Appl. Phys. **80**, 3191 (1996).
16. M.S. Kushwaha, P. Halevi, J. Acoust. Soc. Am. **101**, 619 (1997).
17. J.O. Vasseur, B. Djafari-Rouhani, L. Dobrzynski, P.A. Deymier, J. Phys. Condens. Matter **9**, 7327 (1997).
18. Sajeev John, Phys. Today **40**, 32 (May,1991).
19. R.L. Weaver, Phys. Rev. B **47**, 1077 (1993); R.L. Weaver, Wave Motion **12**, 129 (1990).
20. W.A. Smith. B.A. Auld, IEEE Trans. Ultrason. Ferroelectr. Freq. Control **38**, 40 (1991).
21. W.A. Smith, Proc. SPIE Symp. **1733**, 2 (1992); and references therein.
22. R. Martinez–Sala, J. Sancho, J.V. Sanchez, V. Gómez, J. Llinarez, F. Meseguer, Nature **378**, 241 (1995).
23. M.S. Kushwaha, Appl. Phys. Lett. **70**, 3218 (1997); see also, M.S. Kushwaha, P. Halevi, Jpn J. Appl. Phys. **36**, L 1043 (1997).